Hindawi
Journal of GeoEnergy
Volume 2023, Article ID 4415673, 9 pages
https://doi.org/10.1155/2023/4415673

Research Article

Gas Production Potential in Geothermal-Energy-Enhanced CH_4–CO_2 Swapping Processes

Boyun Guo and Peng Zhang

University of Louisiana at Lafayette, Lafayette, LA, USA

Correspondence should be addressed to Boyun Guo; boyun.guo@louisiana.edu

Received 10 February 2023; Revised 6 May 2023; Accepted 12 May 2023; Published 13 June 2023

Academic Editor: Baojun Bai

Carbon capture and storage has become a practice to reduce the greenhouse effect of carbon dioxide (CO_2) on the global climate. Recent studies have generated increasing concerns about CO_2 leakage from underground structures. This has called for more research on CH_4–CO_2 swapping in natural gas hydrate (NGH) reservoirs to lock CO_2 in a solid state in underground structures. Because the CH_4–CO_2 swapping is too slow to be efficient, this study proposes to use geothermal energy to accelerate the process. This paper presents a technical feasibility analysis of using geothermal energy to assist CH_4–CO_2 swapping for simultaneously storing CO_2 in NGH reservoirs and producing the dissociated natural gas. Mathematical models were developed to compute heat transfer from geothermal zones to NGH reservoirs. A case study was carried out using the data from an NGH reservoir in the Shenhu area, Northern South China Sea. The result of the case study indicates that heat conduction dictates the heat transfer process when the heat convection flow rate is less than 0.01 m^3/s over a heat-releasing borehole length of 2,000 m. Heat convection can significantly accelerate the heat transfer inside the gas hydrate reservoir. The 15°C (designed gas hydrate dissociation temperature in the studied case) heat front will propagate to the upper and lower boundaries of the gas hydrate reservoir (39 ft or 12 m) in 220 days by heat conduction only. This time can be shortened to 140 days with the aid of a fluid convection rate of 0.005 m^3/s. Geothermal heating can significantly increase the initial productivity of wells in heated gas hydrate reservoirs in CO_2 swapping processes. When the gas hydrate reservoir is heated from 6 to 16°C, the fold of increase is expected to exceed five in the studied case. This study shows that CH_4–CO_2 swapping process using geothermal stimulation is a promising method for producing natural gas and locking CO_2 permanently in NGH reservoirs. Further studies should first focus on investigations of the effect of CO_2-hydrate formation on the CO_2 mass transfer inside reservoirs.

1. Introduction

The increasing trend of carbon dioxide (CO_2) level in the atmosphere is a great concern to humankind because of its global warming effect. Many carbon capture and storage projects have been initiated in the past 5 years to place CO_2 in underground structures such as depleted oil reservoirs. Recent studies indicated a high risk of leakage of CO_2 through CO_2-exposed oil wells [1]. The leakage can be due to the loss of sealing integrity of wellbore cement resulting from CO_2–cement interaction over time [2]. According to the computer simulation by Zhang et al. [3], it should take hundreds of years for CO_2 to fully penetrate a 3.5 cm-thick cement sheath through the pore space of cement to reach well casing. But it should take less than a year for CO_2 to fully penetrate a 3.5 cm-thick cement sheath through cracks in the cement. Such cracks in cement sheath were evidenced in careful studies such as that by Duguid et al. [1]. Because the sealing capacity deterioration of wellbore cement sheath is not avoidable, it is logical to "blame" the nature of the high mobility of CO_2 in its supercritical fluid state in the underground storage reservoirs. It is also logical to store the CO_2 in its solid state in low-temperature underground structures such as natural gas hydrate (NGH) reservoirs. This process is called CH_4–CO_2 swapping in previous studies such as that by Cha et al. [4].

A vast amount (10^{15}–10^{18} m^3 at the standard condition) of natural gas is stored in the NGH in the permafrost and offshore sediments [5–7]. The amount of natural gas in the NGH deposits is believed to be greater than that in coal, oil, and conventional gas reservoirs combined [8]. The natural gas in the NGH reservoirs is considered the major source of relatively clean energy to support the future development of the world economy [9–11].

Most of the previous studies on NGH reservoirs have focused on how to produce natural gas from the NGH reservoirs cost-effectively. Three methods have been identified to harvest the natural gas in NGH reservoirs, namely (1) depressurization, (2) thermal stimulation, and (3) the use of hydrate inhibitors. Using the depressurization method, the pressure in the hydrate-bearing zone is lowered below the hydration dissociation pressure at the reservoir temperature [12, 13]. Because NGH is an essential portion of the matrix structure in the reservoir, dissociation of NGH releases water and causes destabilization of the matrix structure. As a result, formation sand production and even wellbore collapse frequently occur during gas production when depressurization is used as a production scheme. With the thermal stimulation method, the temperature of the hydrate-bearing zone is raised above the hydration–dissociation temperature by circulating hot water from the surface [14–16]. This method is very costly due to the power consumption in heating the water. Hydrate inhibitors for gas production from NGH reservoirs include salts and alcohol-type chemicals. They can shift the P–T equilibrium by competing with the NGH for guest and host molecules [17, 18]. This method is also costly due to the use of a large number of expensive inhibitors, especially alcohol-type chemicals. A combination of these methods has been tested to facilitate long-term gas production [19–21]. None of these methods has been proven economical in offshore operations, although some operations are run at a marginal profit in onshore NGH reservoirs in permafrost zones.

CH_4–CO_2 swapping is a process where one CO_2 molecule replaces one CH_4 molecule without destroying the hydrate structure with little water production. The process reduces the possibility of matrix collapse and stratum failure [4]. It is, therefore, more competitive compared with other gas-extraction methods. The process can lock the CO_2 in the reservoir permanently with a low probability of leaking into the atmosphere. However, the swapping efficiency for CH_4 production is low due to the mass transfer barriers caused by the formation of CO_2-hydrates without external energy added to delay the formation of CO_2-hydrates [22].

The recent work of Mahmood and Guo [23] provides a new idea for solving this problem. They proposed a geothermal method for producing natural gas from marine gas hydrate reservoirs. The method uses geothermal energy to accelerate gas hydrate decomposition during the depressurization process. Under the reservoir temperature controlled in a certain range, the thermal energy can accelerate the dissociation of the CH_4-hydrates, delay the formation of CO_2-hydrates, and increase the diffusion coefficient of CO_2. The combination of these three effects is expected to create more diffusion channels to promote CO_2 penetration. The low-level depressurization allows for gas production with manageable sand production and wellbore collapse.

Mahmood and Guo's [23] work considered heat transfer due to conduction only and neglected the effect of gas flow on temperature change inside the reservoir. This left a gap between the reliable heat transfer modeling and well productivity modeling. This gap is filled in the current study using a numerical solution of the diffusion–convection equation to better simulate the heat transfer in the CH_4–CO_2 swapping processes.

2. Heat Transfer Modeling

The heat transfer from a geothermal zone to an NGH reservoir takes two steps: (1) heat transfer from the geothermal zone to a heat-releasing borehole in the NGH reservoir, and (2) heat transfer from the heat-releasing borehole into the NGH reservoir.

Fu et al. [24] proposed a *y*-shaped wellbore configuration and presented an analytical model for heat transfer from a geothermal zone to an NGH reservoir using two horizontal boreholes. The horizontal borehole at the bottom of the geothermal zone is used to receive heat from the geothermal zone, and the horizontal borehole at the top of the NGH reservoir is used for leasing heat into the NGH reservoir. The heat-receiving borehole is designed horizontally to increase heat-receiving efficiency through adequate fluid contact/retention time for heat transfer. An alternative means of improving the heat-receiving efficiency is to use a deeper vertical borehole if drilling technology (thermal-stable drilling fluids) permits. Fu et al.'s [24] system design was modified in this study to replace the horizontal borehole with a vertical borehole in the geothermal zone, assuming it is drillable with the existing drilling fluids. The modified well structure is illustrated in Figure 1. The CO_2 in tank (1) is transferred by compressor (2) to injection well (3), injected through pipe (4) to the bottom of the wellbore in geothermal zone (5), where the CO_2 is heated by geothermal energy. The heated CO_2 in the heat-receiving hole (6) is guided to the heat-receiving hole (7) placed in the NGH reservoir (8). The CO_2 is partially released to the NGH reservoir, and the remaining CO_2 returns to the surface through well tubing (9). The amount of CO_2 released to the NGH reservoir is controlled by the wellhead choke (10) of the gas-producing well (11). The NGH reservoir is heated by the CO_2 stream through heat conduction and heat convection. The released natural gas from the NGH is collected by the gas wellbore (12) and produced through the annulus (13), and processed by the fluid separator (14).

Fu et al.'s [24] study with water as the working fluid demonstrated that the deliverable temperature of the fluid to the heat-receiving borehole is controlled by mainly three factors, including as follows:

(i) Pipe and annular insulation.
(ii) Fluid flow rate.
(iii) Depth of the geothermal zone.

Guo and Zhang [25] presented an analytical model for heat transfer from a horizontal borehole deep into an NGH reservoir by heat conduction only. The model does not

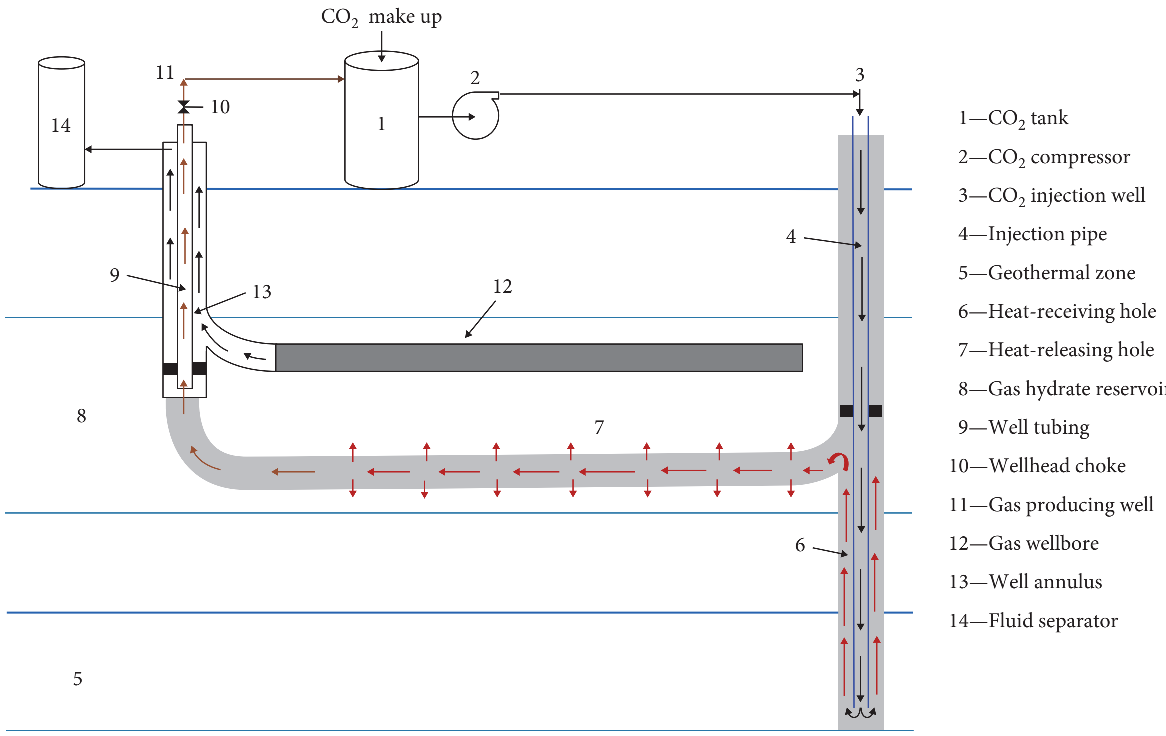

Figure 1: Wellbore configuration for heat transfer from a geothermal zone to an NGH reservoir.

consider heat convection by the fluid flow into the NGH reservoir. The heat transfer process in porous media dominated by heat conduction and heat convection is governed by the following convection–diffusion equation [26]:

$$\phi \frac{\partial T(x,t)}{\partial t} = \alpha \frac{\partial^2 T(x,t)}{\partial x^2} - u \frac{\partial T(x,t)}{\partial x}, \tag{1}$$

where T is the temperature in °C, x is the distance in m, t is time in s, ϕ is porosity in fraction, u is the convective velocity in m/s, and α is the thermal diffusion coefficient defined by the following:

$$\alpha = \frac{k}{\rho c_p}, \tag{2}$$

where k is the thermal conductivity of the solid system in W/(m K), ρ is the density of the solid system in kg/m^3, and c_p is the heat capacity of the solid system in J/(kg K).

The convective velocity is formulated as follows:

$$u = \frac{Q_{in} - Q_{out}}{2\pi x L}, \tag{3}$$

where Q_{in} is the inlet fluid flow rate (injection rate) in m^3/s, Q_{out} is the outlet fluid flow rate (return rate) in m^3/s, x is the radial distance in m, and L is the length of the heat-releasing hole in m.

The diffusion–convection Equation (1) with coefficients defined by Equations (2) and (3) describes heat transfer into the reservoir due to the combined thermal diffusion coefficient of the solid and fluid when α is evaluated considering the contribution of both rock and pore fluid, and u takes the velocity of the injected fluid. This equation is believed adequate for simulating the total heat transfer into the gas hydrate reservoir.

Equation (1) can be solved by the finite difference method (FDM) with the following initial and boundary conditions:

$$T(x,0) = T_0, \tag{4}$$

$$T(r_w,t) = T_w, \tag{5}$$

$$T'(R_+) = T'(R_-), \tag{6}$$

where T_0 is the initial reservoir temperature in °C, r_w is the radius of the heat-releasing borehole in m, T_w is the temperature in the heat-releasing borehole in °C, $T'(R_+)$ is the special derivative of the temperature outside the external boundary in °C/m, and $T'(R_-)$ is the special derivative of the temperature inside the external boundary in °C/m. The profile of the temperature in the heat-releasing borehole (T_w) is given by the analytical model presented by Fu et al. [24]. It is understood that the fluid temperature at any point of the heat-releasing borehole will change with injection time. However, a steady temperature profile is assumed in the whole process. It was noted by Wu et al. [27] that during the flow of CO_2 in vertical and horizontal wellbores, the temperature will be affected by the Joule–Thomson effect and friction heat. However, these effects are not considered in Fu et al.'s [24] analytical model and thus are assumed to be negligible in this study.

With an explicit scheme of formulation of FDM, the discretization of Equation (1) takes the form of

$$\phi \frac{T_i^{n+1} - T_i^n}{\Delta t} = \alpha \frac{T_{i-1}^n - 2T_i^n + T_{i+1}^n}{\Delta x^2} - u \frac{T_i^n - T_{i-1}^n}{\Delta x}, \quad (7)$$

where n is the ordinal of a time spot, i is the ordinal of a grid block, Δx is the length of a grid block, and Δt is the length of a timestep, i.e.,

$$T_i^n = T(x, t), \quad (8)$$

$$T_{i+1}^n = T(x + Dx, t), \quad (9)$$

$$T_{i-1}^n = T(x - Dx, t), \quad (10)$$

$$T_i^{n+1} = T(x, t + Dt). \quad (11)$$

The numerical solution of Equation (7) gives the dynamic distribution of temperature inside the NGH reservoir as follows:

$$T_i^{n+1} = T_i^n + \frac{\Delta t}{\phi} \left(\alpha \frac{T_{i-1}^n - 2T_i^n + T_{i+1}^n}{\Delta x^2} - u \frac{T_i^n - T_{i-1}^n}{\Delta x} \right). \quad (12)$$

3. Gas Well Productivity Modeling

The productivity of the gas production wellbore can be predicted by the analytical model that was originally proposed by Joshi [28]. This model was modified by Guo [29] to include the effects of non-Darcy flow and real gas pseudo-pressure. The model takes the following form:

$$q_g = \frac{k_H h [m(p_e) - m(p_{wf})]}{1{,}424 T_i \left\{ \ln \left[\dfrac{a + \sqrt{a^2 - (\frac{L}{2})^2}}{\frac{L}{2}} \right] + \dfrac{I_{ani} h}{L} \ln \left[\dfrac{I_{ani} h}{r_w (I_{ani} + 1)} \right] + s + D q_g \right\}}, \quad (13)$$

where

$$a = \frac{L}{2} \sqrt{\frac{1}{2} + \sqrt{\left[\frac{1}{4} + \left(\frac{r_{eH}}{\frac{L}{2}} \right)^4 \right]}}, \quad (14)$$

$$I_{ani} = \sqrt{\frac{k_H}{k_v}}, \quad (15)$$

where q_g is the gas production rate in Mscf/day, k_H is the horizontal permeability in mD, k_V is the vertical permeability in mD, h is the thickness of the NGH reservoir in ft, p_e is the reservoir pressure in psi, $m(p_e)$ is the real gas pseudo-pressure at p_e, p_{wf} is the flowing bottom hole pressures in psi, $m(p_{wf})$ is the real gas pseudo-pressure at p_{wf}, T_i is the reservoir temperature in °R, L is the length of the horizontal wellbore in ft, s is the Darcy skin factor, D is the non-Darcy coefficient in day/Mscf, and r_{eH} is the equivalent radius of the drainage area of the horizontal well in ft. The real gas pseudo-pressure is defined as follows and is computed by the spreadsheet developed by Guo and Ghalambor [30]:

$$m(p) = 2 \int_{p_b}^{p} \frac{p}{\mu_g z} dp, \quad (16)$$

where p is pressure in psi, p_b is base pressure in psi, μ_g is gas viscosity in cp, and z is gas compressibility factor.

Because heating the NGH reservoir will increase real gas pseudo-pressure proportionally, the heating effect should not be considered Equation (13). Applying Equation (13) to both nonheated and heated reservoir conditions gives:

$$q_{gNH} = \frac{k_H h [m(p_{eNH}) - m(p_{wfNH})]}{1{,}424 T_i \left\{ \ln \left[\dfrac{a + \sqrt{a^2 - (\frac{L}{2})^2}}{\frac{L}{2}} \right] + \dfrac{I_{ani} h}{L} \ln \left[\dfrac{I_{ani} h}{r_w (I_{ani} + 1)} \right] + s + D q_g \right\}}, \quad (17)$$

$$q_{gH} = \frac{k_H h [m(p_{eH}) - m(p_{wfH})]}{1{,}424 T_i \left\{ \ln \left[\dfrac{a + \sqrt{a^2 - (\frac{L}{2})^2}}{\frac{L}{2}} \right] + \dfrac{I_{ani} h}{L} \ln \left[\dfrac{I_{ani} h}{r_w (I_{ani} + 1)} \right] + s + D q_g \right\}}, \quad (18)$$

Table 1: Basic data for the Shenhu NGH reservoir.

Reservoir top depth	4,415	ft
Pay zone thickness	78	ft
Initial reservoir pressure	2,053	psia
Initial reservoir temperature	43	°F
Design gas wellbore depth	4,445	ft
Design heating-releasing hole depth	4,450	ft
Gas specific gravity (γ_g)	0.55	

Table 2: Parameter values for an interborehole heat transfer model.

Total depth	7,000	m
Wellbore diameter	0.20	m
Inner diameter of cement sheath	0.1397	m
Outer diameter of cement sheath	0.20	m
Outer diameter of pipe	0.089	m
Inner diameter of pipe	0.078	m
Geothermal temperature at top of the vertical section	20	°C
Geothermal gradient	0.0245	°C/m
Thermal conductivity of cement in the heat-receiving borehole	0.1	W/m °C
Thermal conductivity of cement in the heat-releasing borehole	1.5	W/m °C
Thermal conductivity of pipe	45	W/m °C
Fluid flow rate	0.01	m^3/s
Temperature of injected fluid	30	°C
Heat capacity of injected fluid	4,184	J/kg °C
Density of injected fluid	1,000	kg/m^3

Table 3: Basic data for heat transfer analysis.

Density of reservoir rock	2,600	kg/m^3
Porosity of reservoir rock	0.3	
Specific heat of reservoir rock	878	J/kg °C
Thermal conductivity of reservoir	3.06	W/m °C
Initial reservoir temperature	6	°C
Heat-releasing borehole radius	0.1	m
Heat-releasing borehole length	2,000	m
Fluid injection rate	0.01	m^3/s
Fluid return rate	0–0.01	m^3/s
Fluid temperatures at the inlet of the heat-releasing borehole	40	°C
Fluid temperature at the outlet of the heat-releasing borehole	28	°C

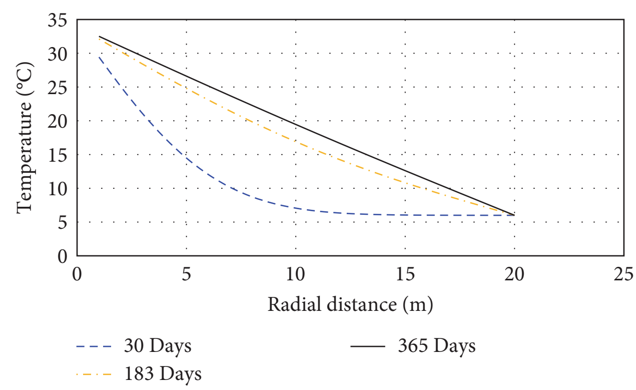

Figure 2: Temperature profiles inside the reservoir with 100% of injected fluid returning to the surface.

where q_{gNH} is the gas production rate of the well in the nonheated NGH reservoir in Mscf/day, p_{eNH} is the driving pressure of the nonheated NGH reservoir in psi, p_{wfNH} is the flowing bottom hole pressure in the nonheated NGH reservoir in psi, q_{gH} is the gas production rate of well in the heated NGH reservoir in Mscf/day, p_{eH} is the driving pressure of the heated NGH reservoir in psi, and p_{wfH} is the flowing bottom hole pressure in the heated NGH reservoir in psi. The driving pressure is defined as the NGH dissociation pressure at a given reservoir temperature. Dividing Equation (18) by Equation (17) gives the following relation:

$$\mathrm{FOI} = \frac{q_{gH}}{q_{gNH}} = \frac{m(p_{eH}) - m(p_{wfH})}{m(p_{eNH}) - m(p_{wfNH})}, \tag{19}$$

where FOI is the fold of increase in well productivity due to reservoir heating in the swapping process.

For NGH reservoirs containing no free gas in the initial conditions (Class 1 W), no gas should flow before the reservoir is depressurized to NGH dissociation pressure. Therefore, the p_{eNH} and p_{eH} are defined as the NGH dissociation pressures at nonheated and heated reservoir conditions. Their values can be determined from the NGH equilibrium curves based on temperature. The p_{wfNH} and p_{wfH} should be selected between the dissociation pressures of CH_4-hydrate and CO_2-hydrate in the swapping process.

4. Case Study

The Shenhu NGH reservoir in the middle of the North Continental Slope of the South China Sea is composed of clayey silt with permeabilities between 1.5 and 7.4 mD [31]. The NGH saturation ranges from 11.7% to 34% [32]. Table 1 provides basic data relevant to well productivity analysis [33, 34].

Table 2 presents a summary of model parameter values for the well structure shown in Figure 1. The result of Fu et al. [24] interwellbore heat transfer model predicted fluid temperatures of 40°C at the inlet and 28°C at the outlet of the heat-releasing borehole.

Table 3 provides basic data relevant to the heat transfer inside the NGH reservoir. Figure 2 presents Equation (12)-calculated temperature profiles for return flow rates of 100% (no fluid flowing into the reservoir). It indicates that the temperature should increase to 6°C at a distance of 20 m from the wellbore in 6 months. Figure 3 shows model-calculated temperature profiles for a return flow rate of 50% (50% of the injected fluid flows into the reservoir). It implies that the

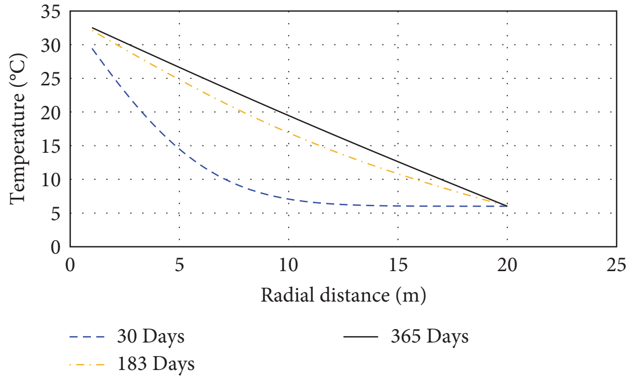

Figure 3: Temperature profiles inside the reservoir with 50% of injected fluid returning to the surface.

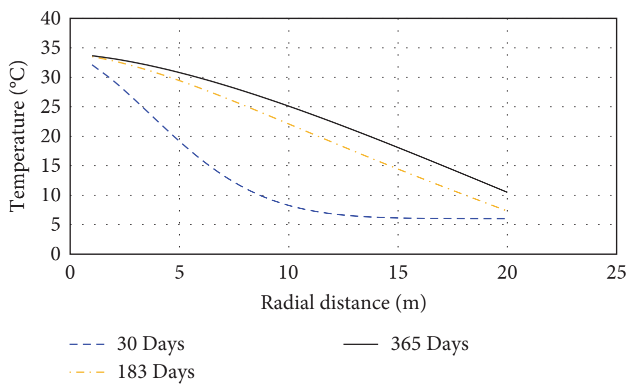

Figure 4: Temperature profiles inside the reservoir with 0% of injected fluid returning to the surface.

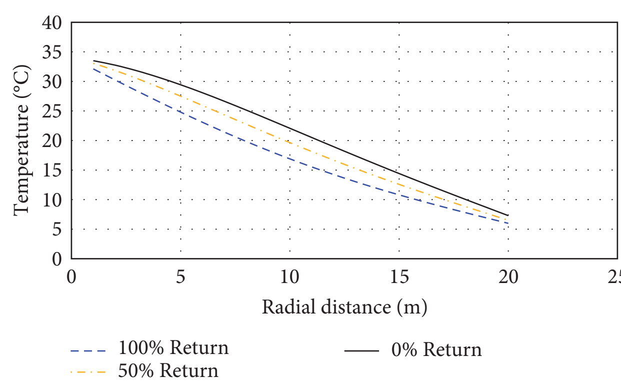

Figure 5: Effect of fluid returning to surface on the temperature profile for injection time of 6 months.

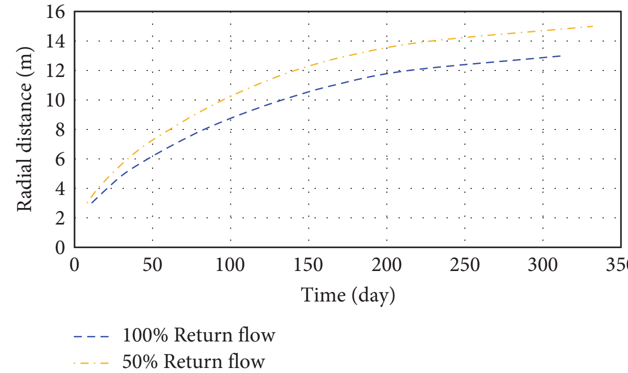

Figure 6: Advancement of the temperature 15°C front.

Table 4: Driving pressures and operating bottom hole pressures at elevated temperatures.

Temperature (°C)	Driving pressure (p_{eH}) (psi)	Flowing bottom hole pressure (p_{wfH}) (psi)
6	650	340
7	720	390
8	810	450
9	910	520
10	1,000	600
11	1,130	680
12	1,240	760
13	1,380	860
14	1,520	960
15	1,685	1,100
16	1,850	1,260

temperature should increase to 6.5°C at a distance of 20 m from the wellbore in 6 months. Figure 4 provides a plot of model-calculated temperature profiles for a return flow rate of 0% (100% of the injected fluid flows into the reservoir). It illustrates that the temperature should increase to 10.5°C at a distance of 20 m from the wellbore in 6 months. Figure 5 shows Equation (12)-calculated effect of fluid flowing into the reservoir on temperature profiles for an injection time of 6 months. It indicates that for a fluid convection flow rate under 0.01 m^3/s, heat conduction is the main mechanism that controls heat transfer inside the reservoir.

Figure 6 presents the calculated propagation front of temperature 15°C as a function of fluid circulation time for two fluid convection levels. It shows that the rate of front propagation decreases with time, which is expected for a radial heat-transfer system. The curves imply that the 15°C front will propagate to the upper and lower boundaries of the gas hydrate reservoir (39 ft or 12 m) in 140 days for a 50% return rate of the injected fluid and in 220 days for the pure heat-conduction condition. If this temperature of 15°C is used for dissociating NGH, the heat convection can significantly accelerate heat transfer and thus the CH_4–CO_2 swapping process.

Figure 7 shows hydrate-phase equilibrium curves for CH_4 and CO_2. Point *A* represents the initial reservoir condition (2,053 psi and 279°K). The line *B*–*C* shows the desired flowing bottom hole pressures and temperatures in geothermal-heated conditions. Coordinates of some points on the gas hydrate dissociation line and the line *B*–*C* are shown in Table 4. Figure 8 plots the fold of increase given by Equation (19), which indicates that a nonlinear relationship exists between the FOI and heated reservoir temperature. The

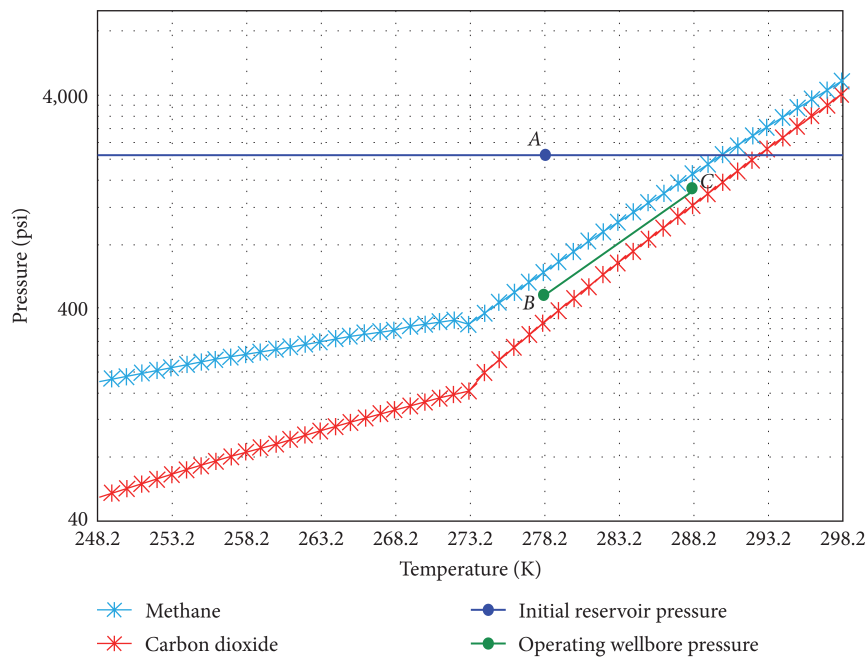

FIGURE 7: Hydrate-phase equilibrium curves for CH_4 and CO_2 (modified from [10]).

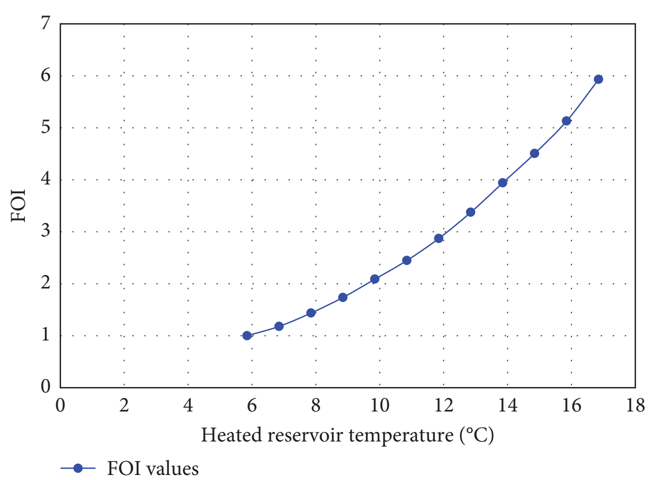

FIGURE 8: Calculated fold of increase in well productivity as a function of heated reservoir temperature.

FOI reaches greater than five at the heated reservoir temperature of about 16°C.

5. Discussion

The accuracy of the result presented in this feasibility analysis is subject to error due to the assumptions made in mathematical modeling. Three issues are discussed here.

First, the mathematical model should overestimate the heat transfer efficiency due to omitted effects: (1) the heat transfer model does not consider the loss of heat to the produced gas, (2) the reservoir temperature drops due to NGH depressurization [13] are not considered, (3) heating of the dissociated gas will cause the gas pressure to increase, which is not considered, (4) Class 1 W hydrate reservoir where there is no free gas in the reservoir in the initial condition, and (5) the formation of CO_2 hydrates should reduce CO_2 mass transfer, which was not studied in this work.

Second, the well productivity model assumes a Class 1 W hydrate reservoir. This should result in underestimated well productivity by the model if the model is applied to other types of gas hydrate reservoirs where free gas exists in the initial condition. Also, it is understood that the well productivity model assumes that the driving pressure is the hydrate dissociation pressure at the external flow boundary of the dissociated region of the reservoir. Because the boundary distance is time-dependent and controlled by heat transfer efficiency, the well productivity should also be fluid-circulation time-dependent.

6. Conclusions

This paper presents a technical feasibility analysis of using geothermal energy to assist CH_4–CO_2 swapping for simultaneously storing CO_2 in NGH reservoirs and producing the dissociated natural gas. Mathematical models were developed to compute heat transfer from geothermal zones to NGH reservoirs. A case study was carried out using the data from an NGH reservoir in the Shenhu area, Northern South China Sea. The following conclusions are drawn:

(i) For the studied gas hydrate reservoir, mathematical modeling of heat conduction and convection shows that heat conduction dictates the heat transfer process when the heat convection flow rate is less than 0.01 m^3/s over a heat-releasing borehole length of 2,000 m.

(ii) Heat convection accelerates heat transfer inside the gas hydrate reservoir. The 15°C (designed gas hydrate dissociation temperature in the studied case) heat front will propagate to the upper and lower boundaries of the gas hydrate reservoir (39 ft or 12 m) in 220 days by heat conduction only. This time can be shortened to 140 days with the aid of a fluid convection rate of 0.005 m^3/s.

(iii) Geothermal heating can significantly increase the initial productivity of wells in heated gas hydrate reservoirs in CO_2 swapping processes. The rate of a fold of increase increases nonlinearly with heated reservoir temperature. When the gas hydrate reservoir is heated from 6 to 16°C, the fold of increase is expected to exceed five in the studied case.

(iv) The accuracy of the result presented in this work is subject to the error due to the assumptions made in mathematical modeling. Future research work should consider heat loss to the produced gas, temperature drops due to NGH depressurization, gas pressure change due to heating, initial free gas in the reservoir, and the effect of formed CO_2 hydrates on CO_2 mass transfer. The well productivity model should be modified to consider the effects of the initial free gas and the dynamic flow boundary due to the dynamic heat transfer process.

In summary, the CH_4–CO_2 swapping process using geothermal stimulation is a promising method for producing natural gas and locking CO_2 permanently in NGH reservoirs. Further studies should first focus on investigations of the effect of CO_2-hydrate formation on the CO_2 mass transfer inside reservoirs.

Nomenclature

c: Specific heat of reservoir rock, J/kg °C
C_p: Heat capacity of the fluid inside the wellbore, J/kg °C
d_c: Inner diameter of insulation-cement sheath, ft
d_p: Inner diameter of pipe, ft
D_c: Outer diameter of insulation-cement sheath, ft
D_p: Outer diameter of pipe, ft
D: Non-Darcy coefficient in day/Mscf
G: Geothermal gradient, °C/ft
h: Reservoir thickness, ft
I_{ani}: Anisotropy index
k_H: Horizontal permeability, mD
k_v: Vertical permeability, mD
K_c: Thermal conductivity of the insulation-cement, W/(m °C)
K_p: Thermal conductivity of insulation pipe, W/(m °C)
L: Length of the horizontal well, ft
$\dot{m}_a$: Fluid flow rate, m^3/s
p: Base pressure, psia
p_e: Reservoir pressure, psia
p_{wf}: Wellbore flowing pressure, psia
p_{eH}: Driving pressure of the heated NGH reservoir, psia
p_{eNH}: Driving pressure of the nonheated NGH reservoir, psia
p_{wfH}: Flowing bottom hole pressure in the heated NGH reservoir, psia
p_{wfNH}: Flowing bottom hole pressure in the nonheated NGH reservoir, psia
q_g: Well production rate, Mscf/day
q_{gNH}: Gas production rate of well in the nonheated NGH reservoir, Mscf/day
q_{gH}: Gas production rate of well in the heated NGH reservoir, Mscf/day
Q_f: Fluid circulation rate, m^3/s
Q_{in}: Inlet fluid flow rate, m^3/s
Q_{out}: Outlet fluid flow rate, m^3/s
r_w: Wellbore radius of laterals, ft
r_{eH}: Radius of drainage area, ft
s: Darcy skin factor
t: Time, s
t_c: Thickness of cement sheath, ft
T: Reservoir temperature, °C
T_i: Initial reservoir temperature, °R
T_f: Temperature of the injected fluid, °C
T_{in}: Inlet temperature, °C
T_{out}: Outlet temperature, °C
u: Convective velocity, m/s
x: Radial distance, m
z: Gas compressibility factor
α: Thermal diffusion coefficient
ϕ: Porosity
ρ: Density of reservoir rock, kg/m^3
γ_g: Gas-specific gravity
μ_g: Gas viscosity, cp.

Data Availability

The data were generated during the study.

Conflicts of Interest

The authors declare that they have no conflicts of interest.

Acknowledgments

This study was supported by BIRD through the project "Safe, sustainable, and resilient development of offshore reservoirs and natural gas upgrading through innovative science and technology: Gulf of Mexico—Mediterranean," award number EC-19 Fossil Energy.

References

[1] A. Duguid, B. Guo, and R. Nygaard, "Well integrity assessment of monitoring wells at an active CO_2-EOR flood," *Energy Procedia*, vol. 114, pp. 5118–5138, 2017.
[2] B. Guo, "Statistical analysis of CO_2 exposed wells to predict long term leakage through the development of an integrated neural-genetic algorithm," University of Louisiana, Lafayette, USA, Report to U.S. DOE project DE FE0009284, May 2017.
[3] P. Zhang, B. Guo, and N. Liu, "Numerical simulation of CO_2 migration into cement sheath of oil/gas wells," *Journal of*

Natural Gas Science and Engineering, vol. 94, Article ID 104085, 2021.
[4] M. Cha, K. Shin, H. Lee, I. L. Moudrakovski, J. A. Ripmeester, and Y. Seo, "Kinetics of methane hydrate replacement with carbon dioxide and nitrogen gas mixture using in situ NMR spectroscopy," *Environmental Science & Technology*, vol. 49, no. 3, pp. 1964–1971, 2015.
[5] K. A. Kvenvolden, "Gas hydrates-geological perspective and global change," *Reviews of Geophysics*, vol. 31, no. 2, pp. 173–187, 1993.
[6] U.S. Geological Survey Fact Sheet 021-01, "Natural gas hydrates—vast resource, uncertain future," USGS, March 2001, https://pubs.usgs.gov/fs/fs021-01/fs021-01.pdf.
[7] J. B. Klauda and S. I. Sandler, "Global distribution of methane hydrate in ocean sediment," *Energy & Fuels*, vol. 19, no. 2, pp. 469-470, 2005.
[8] E. Allison, "Methane hydrates," in *Future Energy: Improved, Sustainable and Clean Options for Our Planet*, T. M. Letcher, Ed., pp. 277–290, Elsevier, 2008.
[9] R. A. Dawe and S. Thomas, "A large potential methane source—natural gas hydrates," *Energy Sources, Part A: Recovery, Utilization, and Environmental Effects*, vol. 29, no. 3, pp. 217–229, 2007.
[10] E. D. Sloan and C. A. Koh, *Clathrate Hydrates of Natural Gases*, CRC Press, Boca Raton, Fla, USA, 3rd edition, 2007.
[11] A. Demirbas, "Methane hydrates as potential energy resource: Part 2—methane production processes from gas hydrates," *Energy Conversion and Management*, vol. 51, no. 7, pp. 1562–1571, 2010.
[12] G. Ahmadi, C. Ji, and D. H. Smith, "Production of natural gas from methane hydrate by a constant downhole pressure well," *Energy Conversion and Management*, vol. 48, no. 7, pp. 2053–2068, 2007.
[13] X.-S. Li, C.-G. Xu, Y. Zhang, X.-K. Ruan, G. Li, and Y. Wang, "Investigation into gas production from natural gas hydrate: a review," *Applied Energy*, vol. 172, pp. 286–322, 2016.
[14] T. Kawamura, M. Ohtake, Y. Sakamoto et al., "Experimental study on steam injection method using methane hydrate core samples," in *Proceedings of the Seventh ISOPE Ocean Mining Symposium*, pp. 83–86, SPE, Lisbon, Portugal, 2007.
[15] G. Li, X. S. Li, L. G. Tang, and Q. P. Li, "Control mechanisms for methane hydrate production by thermal stimulation," in *Proceedings of the 6th International Conference on Gas Hydrates*, pp. 1–10, SPE, Vancouver, BC, Canada, 2008.
[16] H. Najibi, A. Chapoy, H. Haghighi, and B. Tohidi, "Experimental determination and prediction of methane hydrate stability in alcohols and electrolyte solutions," *Fluid Phase Equilibria*, vol. 275, no. 2, pp. 127–131, 2009.
[17] Y. F. Makogon, *Hydrates of Hydrocarbons*, PennWell Publishing Co, Tulsa, OK, 1997.
[18] M. Kurihara, K. Funatsu, H. Ouchi, Y. Masuda, and H. Narita, "Investigation on applicability of methane hydrate production methods to reservoirs with diverse characteristics," in *Proceedings of the 5th International Conference on Gas Hydrates*, vol. 3, pp. 714–725, IAEA, Trondheim, Norway, 2005.
[19] G. J. Moridis and M. T. Reagan, "Strategies for gas production from oceanic Class 3 hydrate accumulations," in *Offshore Technology Conference*, pp. 1–29, OnePetro, Houston, Texas, USA, 2007.
[20] G. J. Moridis and M. T. Reagan, "Gas production from oceanic Class 2 hydrate accumulations," in *Offshore Technology Conference*, pp. 1–8, OnePetro, Houston, Texas, USA, 2007.
[21] G. J. Moridis, T. S. Collett, S. R. Dallimore, T. Satoh, S. Hancock, and B. Weatherill, "Numerical studies of gas production from several CH_4 hydrate zones at the Mallik site, Mackenzie delta, Canada," *Journal of Petroleum Science and Engineering*, vol. 43, no. 3-4, pp. 219–238, 2004.
[22] S. R. Davies, E. D. Sloan, A. K. Sum, and C. A. Koh, "In situ studies of the mass transfer mechanism across a methane hydrate film using high-resolution confocal Raman spectroscopy," *The Journal of Physical Chemistry C*, vol. 114, no. 2, pp. 1173–1180, 2010.
[23] M. N. Mahmood and B. Guo, "Gas production from marine gas hydrate reservoirs using geothermal-assisted depressurization method," *Advances in Geo-Energy Research*, vol. 7, no. 2, pp. 90–98, 2023.
[24] C. Fu, B. Guo, L. Shan, and J. Lee, "Mathematical modeling of heat transfer in y–shaped well couples for developing gas hydrate reservoirs using geothermal energy," *Journal of Natural Gas Science and Engineering*, vol. 96, Article ID 104325, 2021.
[25] B. Guo and H. Zhang, "Mathematical modeling of the dynamic temperature profile in geothermal-energy-heated natural gas hydrate reservoirs," *Sustainability*, vol. 14, no. 5, Article ID 2767, 2022.
[26] F. P. Incropera, D. P. DeWitt, T. L. Bergman, and A. S. Lavine, *Fundamentals of Heat and Mass Transfer*, John Wiley & Sons, Hoboken, NJ, 6th edition, 2007.
[27] L. Wu, Z. Luo, L. Zhao, N. Zhang, Z. Yao, and Y. Jia, "Transient temperature-pressure field model of supercritical CO_2 fracturing wellbore with tubing and annulus co-injection," *Greenhouse Gases: Science and Technology*, vol. 12, no. 1, pp. 85–102, 2022.
[28] S. D. Joshi, "Augmentation of well productivity with slant and horizontal wells (includes associated papers 24547 and 25308)," *Journal of Petroleum Technology*, vol. 40, no. 6, pp. 729–739, 1988.
[29] B. Guo, *Well Productivity Handbook*, Elsevier, Cambridge, 2nd edition, 2019.
[30] B. Guo and A. Ghalambor, *Natural Gas Engineering Handbook*, Gulf Publishing Company, Houston, 2nd edition, 2012.
[31] C. Liu, Y. Ye, Q. Meng et al., "The characteristics of gas hydrates recovered from Shenhu area in the South China Sea," *Marine Geology*, vol. 307–310, pp. 22–27, 2012.
[32] T. Yu, G. Guan, D. Wang, Y. Song, and A. Abudula, "Numerical evaluation on the effect of horizontal-well systems on the long-term gas hydrate production behavior at the second Shenhu test site," *Journal of Natural Gas Science and Engineering*, vol. 95, Article ID 104200, 2021.
[33] M. Su, R. Yang, and N. Y. Wu, "Structural characteristics in the Shenhu area, northern continental slope of South China Sea, and their influence on gas hydrate," *Acta Geologica Sinica*, vol. 88, pp. 318–326, 2014.
[34] E. Ekhator and B. Guo, "Assessing the effect of well completion types on productivity in a Class 1G gas hydrate reservoir under pseudo steady state," *Petroleum*, vol. 7, no. 4, pp. 414–426, 2021.